Colloid Polym Sci 278:946–953 (2000)


ORIGINAL CONTRIBUTION

T. Ogasawara
A. Nara
H. Okabayashi
E. Nishio
C. J. O'Connor

# Time-resolved near-infrared and two-dimensional near-infrared correlation spectroscopic studies on polymerization of the silane coupling agent perfluorooctyltrimethoxysilane

Received: 23 November 1999
Received in Revised form: 23 February 2000
Accepted 4 March 2000

T. Ogasawara · H. Okabayashi (✉)
Department of Applied Chemistry
Nagoya Institute of Technology
Gokiso-cho, Showa-ku
Nagoya 466-8555, Japan

A. Nara · E. Nishio
Nicolet Japan, Osaka Laboratory
Terauchi, Toyonaka
Osaka 560-0872, Japan

C. J. O'Connor
Department of Chemistry
The University of Auckland
Private Bag 92019, Auckland
New Zealand

**Abstract** The polymerization behavior of perfluorooctyltrimethoxysilane (PFOS) in ethanol, which is acid-catalyzed by 0.25 M HCl, has been examined using time-resolved near-IR and 2D near-IR correlation spectra. In the time-resolved near-IR spectra, the bands at 5164 and 4825 $cm^{-1}$ have been assigned to the combination bands of water and ethanol OH groups, respectively. It has been found that the absorbance variation of the two near-IR bands occurs in a two-step process. The absorbance of the 5164 $cm^{-1}$ band rapidly decreases in the initial step but increases exponentially in the second step, while that of the 4825 $cm^{-1}$ band rapidly increases both in the initial step and, exponentially, in the second step. These results indicate that the time-dependent absorbance variation of the two near-IR bands reflects the polymerization process of PFOS, in which consumption and release of water molecules and release of methanol in the two-step process occur as a consequence of the acid-catalyzed hydrolysis of methoxy groups and the formation of silanols (SiOH) to form a siloxane bond. It has also been found that this polymerization process is distinctly reflected in the 2D near-IR correlation spectra.

**Key words** Time-resolved near infrared · Two-dimensional correlation · Perfluorooctyltri methoxysilane · Condensation water, alcohol and silanol behavior

## Introduction

Alkyl alkoxides [$(R\mathrm{Si}(\mathrm{O}R')_3$, $R$ = alkyl, $R'$ = methyl or ethyl groups)] have been used extensively to reinforce interface between a fiber and a resin or between two different substrates through chemical interaction with silane molecules [1–4]. The mechanism responsible for the improved adhesion of this particular reinforcement has not yet been completely clarified, although many attempts [5–10] have been made to elucidate it.

It is well known that, of the many alkyl alkoxides, perfluorooctyltrimethoxysilane (PFOS) is a representative of the silane coupling agents which can be used to control the wettability of the surface of materials. The microstructure of the PFOS layer, coated onto the surface of substrates, should play an important role in the characteristic appearance of the surface. We may assume that the perfluorooctyl chains, as well as the siloxane-polymer portions, self-assemble during polymerization of the PFOS-substrate system, since the perfluorooctyl portion has both hydrophobic and lipophobic characteristics [11]. Thus, the self-assembling behavior of the PFOS chains must affect the microstructure of the PFOS layer.

In a previous study [12], we used 2D near IR (NIR) correlation spectroscopy to examine the behavior of each of the $NH_2$, silanol OH, water OH and ethanol OH groups during polymerization of 3-aminopropyltriethoxysilane (APTS), initiated by water molecules in ethanol. The results showed that the NIR band at 5184 $cm^{-1}$,

coming from the so-called $\nu_2 + \nu_3$ combination mode of water, decreases in absorbance as a consequence of hydrolysis and simultaneously shifts downwards in a two-step process as the reaction proceeds. In particular, it has been assumed from this downward shift that variation in the hydrogen-bonding environment of water molecules, which can be reduced to the $NH_2$ group of APTS, occurs during the polymerization. Furthermore, it has also been found that this process is strongly reflected in the 2D NIR correlation spectra.

In this present study, we use time-resolved NIR and 2D NIR correlation spectroscopy [13–22] in order to examine the dynamic behavior of the PFOS–ethanol–HCl·$H_2O$ system. Since the perfluorooctyl segment of a PFOS molecule has no interaction with water molecules, owing to its characteristics of both hydrophobicity and lipophobicity, we may therefore expect that the behavior of water and ethanol in this system should be different from that in the APTS–ethanol–water system.

## Experimental

### Materials

PFOS was purchased from Shinetsu Chemical Industry and was used without further purification. A PFOS–ethanol–0.25 M HCl·$H_2O$ (1:1:0.4 weight ratio) solution was used to follow the condensation reaction between PFOS molecules. For the PFOS–ethanol–0.25 M HCl·$H_2O$ system, a transparent one-phase solution was obtained 35 s after mixing the sample. Two hours later, this transparent solution changed into a two-phase solution. The $^1H$ NMR spectra (not shown) provided evidence that the upper transparent layer and the bottom viscous, turbid layer are solvent-rich and polymer-rich, respectively.

### Methods

Time-resolved NIR spectra of the sample one-phase solution sandwiched between two $CaF_2$ windows using Pb spacers (0.5 mm) were recorded, until phase separation occurred, at a resolution of 8 $cm^{-1}$ on a Nicolet Magna System 860 Fourier transform IR spectrometer (4000–10000 $cm^{-1}$) equipped with a DTGS KBr detector. Forty scans were accumulated to ensure an acceptable signal-to-noise ratio.

Synchronous and asynchronous 2D NIR correlation spectral maps were calculated from the time-resolved NIR spectral data, using the program (2D-Pocha) for generalized 2D correlation spectroscopy.

### Background of 2D NIR correlation spectroscopy

Noda [13–16] proposed a method for analysis of a generalized 2D correlation spectrum and described its theoretical background and application. We summarize this here.

The time-dependent intensity (absorption) of an IR spectrum measured at a wavenumber, $\nu$, under a small perturbation can be expressed as a combination of two components [15]

$$A(\nu, t) = \tilde{A}(\nu) + \tilde{A}(\nu, t) \ , \tag{1}$$

where the first term, $\tilde{A}(\nu)$, is the absorbance of a system observed without the perturbation and the second term, $\tilde{A}(\nu, t)$, is that of a system induced by perturbation.

For the time-dependent intensities, $\tilde{A}(\nu_1, t)$ and $\tilde{A}(\nu_2, t)$, of the IR signals, which are measured at two different wavenumbers, the intensity cross-correlation function, $X(\tau)$, is defined as follows.

$$X(\tau) = \lim_{\tau \to \infty} \frac{1}{T} \int_{-T/2}^{T/2} \tilde{A}(\nu_1, t)\tilde{A}(\nu_2, t + \tau)\mathrm{d}t \ , \tag{2}$$

When we assume that the molecular level variations in the system, which alter the IR spectrum, respond linearly to the perturbation, it is expected that the time-dependence of the IR signal is expressed by the following equation,

$$A(\nu, t) = A'(\nu) \sin \omega t + A''(\nu) \cos \omega t \ . \tag{3}$$

By substituting Eq. (3) into Eq. (1), the function $X(\tau)$ reduces to

$$X(\tau) = \Phi(\nu_1, \nu_2) \cos \omega t + \Psi(\nu_1, \nu_2) \sin \omega \tau \ . \tag{4}$$

We may regard the functions $\Phi(\nu_1, \nu_2)$ and $\Psi(\nu_1, \nu_2)$, as the real and imaginary components of the cross-correlation function, which are referred to as the synchronous and asynchronous 2D IR correlation intensities, respectively.

The synchronous correlation intensity, $\Phi(\nu_1, \nu_2)$, characterizes the degree of coherence between time-dependent variations of IR signals measured at two different wavenumbers. The magnitude of $\Phi(\nu_1, \nu_2)$ becomes nonvanishing only if the time-dependent intensity variations of the two IR signals are similar to each other. Conversely, the asynchronous correlation intensity, $\Psi(\nu_1, \nu_2)$, characterizes the independent and uncoordinated intensity variations of the IR signals. The magnitude of $\Psi(\nu_1, \nu_2)$ becomes nonvanishing only if the time-dependent variations are not synchronized.

We can obtain the 2D IR spectra by plotting these correlation intensities over a spectral plane, which is defined by the two orthogonal wavenumber axes, $\nu_1$ and $\nu_2$.

In a synchronous 2D NIR correlation spectrum [17–22], the autocorrelation peaks (or autopeaks) on the diagonal line represent the extent of the dynamic intensity variation of spectral bands with different wavenumbers. For the cross-peak, whose spectral coordinates are observed at two different wavenumbers, with similar tendencies for dynamic variation in intensity, synchronous cross-peaks appear at off-diagonal positions. When the intensities of the two bands with different wavenumbers are simultaneously either increasing or decreasing, the cross-peaks are positive, while, when the intensity of one band is increasing while that of the other band is decreasing, the cross-peaks are negative (usually shaded).

In an asynchronous 2D NIR correlation spectrum, which consists only of off-diagonal cross-peaks, the cross-peaks and their signs directly reflect the difference between the time-dependent sequential variations of NIR band intensities [13, 14]. When the tendency for dynamic intensity variation of cross-peaks with two different coordinates is dissimilar, then the cross-peaks appear in the asynchronous spectrum. This characteristic makes it possible to enhance the spectral resolution of highly superimposed NIR bands. In particular, we emphasize that we can assign the specific sequence for an increase or a decrease in intensity occurring at different times. For example, in the asynchronous spectrum, a shaded cross-peak indicates that the intensity variation (increase or decrease) for the band at wavenumber $\nu_1$ occurs later compared with that of the band at wavenumber $\nu_2$. An unshaded cross-peak indicates the opposite effect, i.e., the intensity variation occurs sooner.

## Results and discussion

It is well known that the acid- or base-catalyzed hydrolysis of alkoxide or alkyl alkoxide in alcohol solution results in the formation of silanols which

subsequently condense to form polymers and that the nature of the produced polymer species is different in acid- and base-catalyzed products [23]. This difference can be explained mainly by differences in the relative rates of hydrolysis of the alkoxide or alkyl alkoxide groups to form silanols (Eq. 1), condensation of silanols to form polymers (Eq. 2) and linking of the polymeric species [23]. The relative rates of these three reactions depend on the concentrations of water and the alkoxide or alkyl alkoxide and the pH of the solution.

The acid-catalyzed polymerization of PFOS may be expressed by the following reaction schemes [24–26].

$$F(CF_2)_6CH_2CH_2SiL_2(OCH_3) + H_2O \xrightarrow{HCl} F(CF_2)_6CH_2CH_2SiL_2(OH) + CH_3OH \quad (5)$$

$$2F(CF_2)_6CH_2CH_2SiL_2(OH) \longrightarrow F(CF_2)_6CH_2CH_2Si(L_2)\text{—}O\text{—}Si(L_2)CH_2CH_2(CF_2)_6F + H_2O \quad (6)$$

$L = \text{—}OCH_3, \text{—}OH$ or $\text{—}O\text{—}Si$

In this present study, time-resolved NIR spectra of the PFOS–ethanol–0.25 M $HCl{\cdot}H_2O$ solution were measured until phase separation occurred in the sample solution, and the behavior of the water, silanol and methanol released during the polymerization process were examined separately.

## Time-resolved NIR spectra of the polymerization process

NIR spectra of the PFOS–ethanol–0.25 M $HCl{\cdot}H_2O$ system in the 4000–7500 $cm^{-1}$ region are shown in Fig. 1 together with the NIR spectrum of liquid PFOS. The band at 5164 $cm^{-1}$ arises from water molecules and is assigned to the combination modes ($\nu_2 + \nu_3$) between the $H_2O$ deformation mode ($\nu_2$) and the $H_2O$ asymmetric stretch mode ($\nu_3$) [27]. The band at 6837 $cm^{-1}$ may be assigned to the combination mode ($\nu_1 + \nu_3$) between a $H_2O$ symmetric stretch mode ($\nu_1$) and a $\nu_3$ mode and that at 4829 $cm^{-1}$ to the combination mode between the alcohol OH stretch and bend modes of the added ethanol and of methanol released as a consequence of hydrolysis. The shoulder band at 5300 $cm^{-1}$ is assigned to the combination modes between the silanol OH stretch mode and the overtone of the SiOH bend mode [28]. The broad bands at 6200–6400 and 6837 $cm^{-1}$ also come from the overtone modes of alcohol and water OH groups.

It has been found that the absorbances of the NIR bands at 5164 and 4829 $cm^{-1}$, as well as those at 6837 and 6200–6400 $cm^{-1}$, strongly depend upon reaction

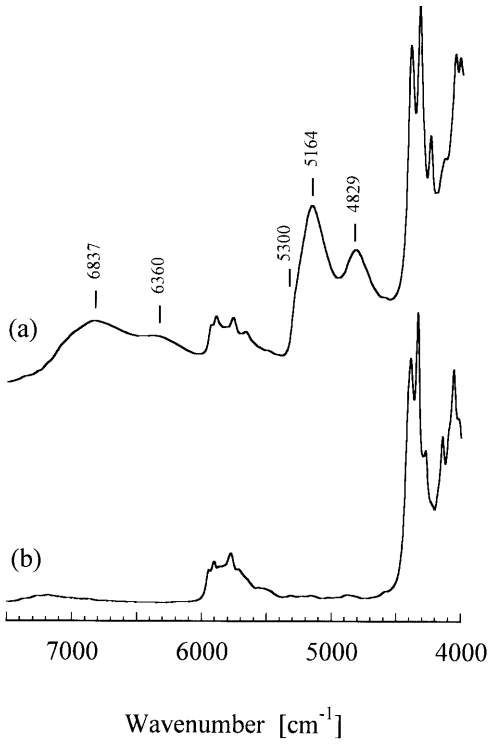


**Fig. 1** Near-IR (*NIR*) spectra of the perfluorooctyltrimethoxysilane (*PFOS*)–ethanol–0.25 M $HCl{\cdot}H_2O$ system (*a*) and liquid PFOS (*b*)

time, although the extent of absorbance variation is very small (0.055 for the 5164 $cm^{-1}$ band and 0.026 for the 4829 $cm^{-1}$ band), implying that the time dependence of absorbance for these bands reflects the rates of these reaction (i.e., those of hydrolysis and condensation).

The time dependence of absorbance for the 5164 and 4829 $cm^{-1}$ bands are shown in Fig. 2A and B, respectively. For the time-resolved 5164 $cm^{-1}$ band (Fig. 2A), it is found that variation in absorbance occurs in a two-step process (I and II), (although the extent of variation is small). That is, the absorbance rapidly decreases in the initial step (I) (12 min) and, in the second step (II), the intensity increases exponentially until it becomes almost constant some 200 min later. Similar time-dependence was found for the absorbance of the 6837 $cm^{-1}$ band. The absorbance variation of the bands at 5164 and 6837 $cm^{-1}$ indicates that in the initial step water molecules are utilized for hydrolysis of methoxy groups, while in the second step, water molecules are released in the condensation reaction to form a siloxane bond.

Since the NIR bands at 5300 and 5164 $cm^{-1}$ are superimposed upon each other (Fig. 1) and the time-dependent absorbance data for the 5300 $cm^{-1}$ band are extremely small and are not easily distinguished from those for the 5164 $cm^{-1}$ band, the kinetics of their variation cannot be analyzed.

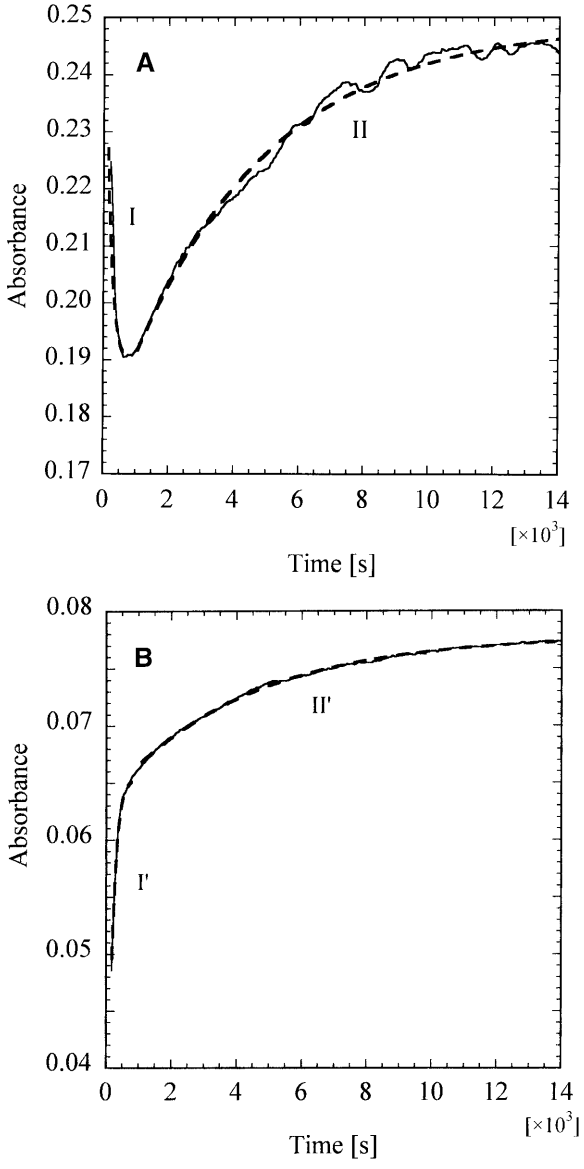


**Fig. 2** Time-dependence of absorbance for **A** the 5164 and **B** the 4829 $cm^{-1}$ bands (*solid line*) and the best-fit curves for **A** the 5164 and **B** the 4829 $cm^{-1}$ bands (*broken lines*) for the PFOS–ethanol–0.25 M $HCl \cdot H_2O$ system

From the time-dependence of absorbance for the band at 4829 $cm^{-1}$ (Fig. 2B), it is evident that the release of methanol also occurs in a two-step (I′ and II′) process. An initial step, I′, and a second step, II′, correspond well to steps I and II, respectively, for the time-dependent absorbance data of the 5164 $cm^{-1}$ band (Fig. 2A). We may therefore assume that the release of methanol occurs rapidly in the initial step and that these time-dependent data for absorbance reflect the kinetics of hydrolysis and condensation in the PFOS–ethanol–0.25 M $HCl \cdot H_2O$ system.

## Kinetics and mechanism of the polymerization process

A kinetics analysis of the absorbance data for the I (or I′) and II (or II′) processes of the 5164 $cm^{-1}$ and 4829 $cm^{-1}$ bands was carried out, after assuming that the rate of variation of the band intensity for each step follows a first-order reaction (Fig. 2, broken lines). The rate constants thus obtained are $k^{I} = 6.23 \times 10^{-3}\,s^{-1}$ (process I) and $k^{II} = 2.35 \times 10^{-4}\,s^{-1}$ (process II) for the 5164 $cm^{-1}$ band and $k^{I'} = 6.64 \times 10^{-3}\,s^{-1}$ (process I′) and $k^{II'} = 2.42 \times 10^{-4}\,s^{-1}$ (process II′) for the 4829 $cm^{-1}$ band. The rate constants $k^{I}$ and $k^{II}$ thus correspond well to the $k^{I'}$ and $k^{II'}$ values, respectively.

In a previous paper [29], we demonstrated the results of small-angle X-ray scattering (SAXS) time-resolved on a short time scale for the acid-catalyzed condensation reaction of PFOS in ethanol. The time-dependence of the apparent radius of gyration, obtained from the Guinier plots, showed that the growth of the PFOS polymer precursors occurs in a two-step process, within 2 h for PFOS, in which small clusters involving monomers, dimers and trimers are formed in the initial step and the formation of larger clusters occurs in the second step. In the SAXS study, 10-min SAXS measurements were repeated after appropriate time intervals.

However, in this present study, the time scale of the NIR measurements was very short, since it takes about 50 s to obtain one NIR spectrum; therefore, we may assume that formation of dimers predominates in the initial step (I and I′) and that larger clusters, such as trimers and tetramers, are preferentially produced in the second step (II and II′).

## 2D NIR correlation spectra of the PFOS–ethanol–acidic water system

The 2D NIR correlation spectra of the PFOS–ethanol–0.25 M $HCl \cdot H_2O$ system are shown in Figs. 3 and 4. In the synchronous correlation spectrum (Fig. 3A), which was calculated from the NIR spectral data time-resolved for the first 12 min of reaction, we find a positive autocorrelation peak at the diagonal position of coordinate A(5165, 5165) and two negative cross-peaks at the off-diagonal positions of coordinates B(5165, 4800) and D(4800, 5165). The synchronous spectrum (Fig. 3B), which was calculated from the NIR data time-resolved for the time period 12–212 min, provides two positive autocorrelation peaks at coordinates (5165, 5165) and (4825, 4825) and two positive cross-peaks at coordinates (5165, 4825) and (4825, 5165). We can construct a synchronous correlation square by connecting the two autopeaks and the two cross-peaks, which implies that there is a correlation between the two NIR bands at 5165 and 4825 $cm^{-1}$, which come from the $\nu_2 + \nu_3$

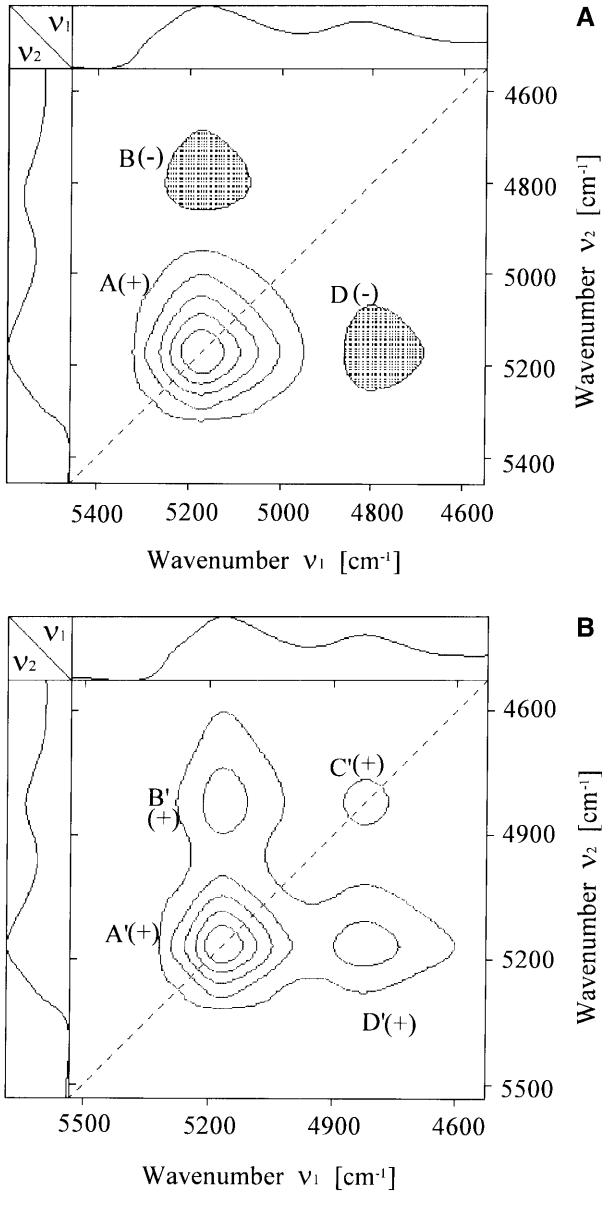


**Fig. 3** Synchronous correlation spectra of the PFOS–ethanol–0.25 M $HCl \cdot H_2O$ system (**A** calculated from the NIR spectral data time-resolved during the first step and **B** calculated from the NIR spectral data time-resolved during the second step). + and – identify the positive and negative peaks, respectively

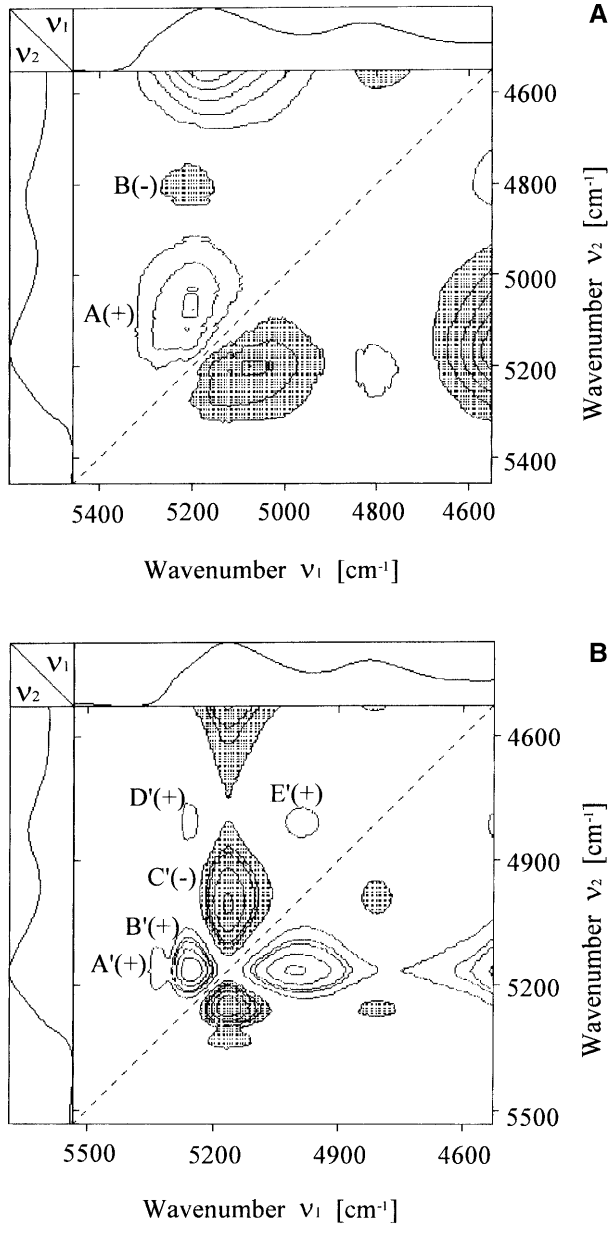


**Fig. 4** Asynchronous correlation spectra of the PFOS–ethanol–0.25 M $HCl{\cdot}H_2O$ system (**A** calculated from NIR spectral data time-resolved during the first step and **B** calculated from the NIR spectral data time-resolved during the second step). + and – identify the positive and negative peaks, respectively. $A'(\nu_1 = 5340, \nu_2 = 5169)$, $B'(\nu_1 = 5253, \nu_2 = 5169)$, $C'(\nu_1 = 5169, \nu_2 = 4987)$, $D'(\nu_1 = 5253, \nu_2 = 4820)$, $E'(\nu_1 = 4987, \nu_2 = 4820)$

combination modes of a $H_2O$ molecule and from the combination mode of alcohol.

It should be noted that there is a marked difference in the sign of the cross-peaks between the synchronous correlation maps (Fig. 3A, B): in Fig. 3A the sign of the cross-peak B is negative, while in Fig. 3B that of the peaks B and C is positive. We may interpret this difference on the basis of the time-resolved NIR results, i.e. the absorbance of the 5164 $cm^{-1}$ band rapidly decreases in the first 12 min of the reaction, while that of the 4825 $cm^{-1}$ band rapidly increases during this period. Accordingly, the positive sign of autopeak A reflects a decrease in the absorbance of the 5165 $cm^{-1}$ band, while the negative cross-peak B reflect the rapid increase in the amount of methanol released as a consequence of the initial acid-catalyzed hydrolysis reaction. In the synchronous correlation map (Fig. 3B), which

was calculated from the time-resolved NIR spectral data during the second stage of the reaction (12–212 min), only two positive cross-peaks (B′ and D′) are found in addition to two positive autopeaks (A′ and C′) (i.e., no negative peaks), reflecting the releases of both water and methanol as a consequence of hydrolysis and condensation in the second step.

Asynchronous 2D NIR correlation maps of the same sample system were calculated from the data in the initial step and in the second step (Fig. 4A, B). In the asynchronous correlation analysis, it should be emphasized that enhancement of the spectral resolution makes it possible to separate the superimposed bands into individual components [13, 14]. Indeed, in the time-resolved NIR data of the present system, we were able to separate superimposed bands.

In the asynchronous correlation map (Fig. 4A), calculated from the time-resolved data for the first 12 min, cross-peaks A and B are found at coordinates (5200, 5072) and (5200, 4800). The contour level of cross-peak A is extended from $\nu_1 = 5100\,\mathrm{cm}^{-1}$ to $\nu_1 = 5350\,\mathrm{cm}^{-1}$ and from $\nu_2 = 4900\,\mathrm{cm}^{-1}$ to $\nu_2 = 5200\,\mathrm{cm}^{-1}$, implying that the 5300 $\mathrm{cm}^{-1}$ band coming from silanol groups, in addition to the combination band arising from water molecules, also contributes to the extended contour level of cross-peak A. Since the intensity of the asynchronous correlation directly reflects the difference in the extent of the time dependence of the intensity between the two bands, the sign and the intensity of these cross-peaks should reflect the difference in the time-dependent behavior of water, silanol and alcohol in the polymerization process. Therefore, the positive cross-peak A and the negative cross-peak B (Fig. 4A) obviously reflect that the absorbance of the band extended over the large area of $\nu_1 = 5100$–$5350$ and $\nu_2 = 4900$–$5200\,\mathrm{cm}^{-1}$ rapidly decreases in the first 12 min, while that of the band at about 4800 $\mathrm{cm}^{-1}$ rapidly increases as a consequence of alcohol release.

In the asynchronous correlation map (Fig. 4B), which was calculated from the NIR spectral data time-resolved in the range of the second step, enhancement of the spectral resolution brings about marked separation of superimposed bands. The appearance of the cross-peaks A′, B′, C′, D′ and E′, separated by the resolution enhancement, imply that at least four NIR bands appear in the 4900–5500 $\mathrm{cm}^{-1}$ region during the second step. The two cross-peaks A′ and B′ at coordinates (5340, 5169) and (5253, 5169) may come from the NIR bands at 5340 and 5253 $\mathrm{cm}^{-1}$ of the silanol (SiOH) groups, which may be assigned to the combination modes ($\nu + 2\delta$) between the silanol OH stretch mode ($\nu$) and the overtone mode ($2\delta$) of the SiOH bend mode ($\delta$). We may ascribe the 5340 and 5253 $\mathrm{cm}^{-1}$ bands to weakly associated and associated silanol groups, respectively.

Shih and Koenig [30] found Raman bands at 3625 and 3702 $\mathrm{cm}^{-1}$ for hydrolyzed trimethylchlorosilane, which were assigned by Batuev et al. [31] to the vibrations of unassociated and associated SiOH groups, respectively. They also found Raman bands at 834 and 880 $\mathrm{cm}^{-1}$ and assigned the latter band to the SiOH bend mode. The 834 $\mathrm{cm}^{-1}$ band probably comes from the bend mode of associated SiOH groups, although did not describe the assignment of this band. If we take the IR data of silica, which were examined by Benesi and Jones [32] and by Richards and Thompson [33], into account, we may assume that the bend modes of the associated SiOH groups are in the 830–880 $\mathrm{cm}^{-1}$ region and that their wavenumber strongly depends upon the strength of the hydrogen bonds.

In the IR spectrum of the PFOS–ethanol–0.25 M $HCl{\cdot}H_2O$ system, we have confirmed the presence of the very weak and broad shoulder bands at 3600–3680 $\mathrm{cm}^{-1}$ (spectrum not shown), in which the OH stretch band (3660 $\mathrm{cm}^{-1}$) of the weakly associated silanol and that (3620 $\mathrm{cm}^{-1}$) of associated silanol are superimposed upon each other. If we assume that superimposition of the two $\nu^{\mathrm{SiOH}}$(OH) bands at 3620 and 3660 $\mathrm{cm}^{-1}$ provides the shoulder band at 3600–3680 $\mathrm{cm}^{-1}$ and that the bend modes ($\delta$) of the SiOH groups, which furnish the 3620 and 3660 $\mathrm{cm}^{-1}$ bands, appear at 834 and 880 $\mathrm{cm}^{-1}$, respectively, then we expect the wavenumbers of the combination ($\nu + 2\delta$) bands as listed in Table 1. Thus, we may assign the two cross-peaks A′ and B′ to weakly associated and associated silanol groups, respectively.

Formation of weakly associated and associated SiOH groups in the second step may be caused by giant aggregates which are formed in the second step because of the hydrophobic and lipophobic nature of the bulky alkyl groups [29]. The steric hindrance of such bulky alkyl groups promotes isolation of any silanol groups which may be incorporated into the grooves of the aggregates of the perfluorooctyl chains and their envi-

**Table 1** Combination ($\nu + 2\delta$) bands expected for the fundamental $\nu^{\mathrm{SiOH}}$ (OH) and $\delta$ modes for SiOH

| | Observed ($\mathrm{cm}^{-1}$) | | Combination ($\nu + 2\delta$) ($\mathrm{cm}^{-1}$) | | $\Delta(\mathrm{cm}^{-1})$[a] |
|---|---|---|---|---|---|
| | $\nu^{\mathrm{SiOH}}$(OH) | $\delta$(SiOH) | Expected | Observed | |
| Perfluorooctyltrimethoxysilane–ethanol–0.25 M $HCl{\cdot}H_2O$ | 3660 | 880 | 5420 | 5340 | 80 |
| | 3620 | 834 | 5288 | 5253 | 35 |

[a] $\Delta(\mathrm{cm}^{-1}) = (\nu + 2\delta)_{\mathrm{expected}} - (\nu + 2\delta)_{\mathrm{observed}}$

ronment may be close to the hydrophobic and lipophobic regions, bringing about formation of the weakly associated silanols; however, most of the silanol groups, which belong to the associated SiOH groups, probably form a hydrogen-bond network with SiOH itself, or water or ethanol molecules.

The positive signs of the cross-peaks A′ and B′ imply that an increase in absorbance of the water band at 5169 $cm^{-1}$ occurs more slowly than the increase in absorbance of the bands at 5340 and 5253 $cm^{-1}$. The intensity of the B′ cross-peaks is greater than that of the A′ peaks, revealing that the time dependence of the absorbance of the 5169 $cm^{-1}$ band occurs predominantly in the second step.

The negative cross-peak, C′, at coordinates (5169, 4987) obviously comes from water molecules which participate in the strong hydrogen-bonding system. From the negative sign of this cross-peak, we may assume that the increase in absorbance of the 4987 $cm^{-1}$ band occurs prior to that of the 5169 $cm^{-1}$ band.

The appearance of the positive cross-peak, D′, implies that a correlation exists between the 5253 and 4820 $cm^{-1}$ bands and that the absorbance variation of the 4820 $cm^{-1}$ band occurs more slowly than that of the methanol band at 5253 $cm^{-1}$. For the cross-peak, E′, it is evident that there is a correlation between the 4987 and 4820 $cm^{-1}$ bands and that the increase in intensity of the latter band occurs more slowly than that of the former band.

Thus, in the asynchronous correlation map (Fig. 4B), which reflects the second step, II or II′, in the polymerization process, the time-dependence of the absorbance of the 5169 $cm^{-1}$ band predominantly occurs in the NIR data time-resolved during the second step and the absorbance variation of the 5169 $cm^{-1}$ band occurs more slowly than that of the 5253 $cm^{-1}$ band.

## Conclusion

Time-resolved NIR spectra of the PFOS–ethanol–0.25 M $HCl{\cdot}H_2O$ system were examined. The absorbance variation in the two regions 4500–5500 and 6000–7000 $cm^{-1}$, in which the combination modes of the silanol group, water molecules and alcohol appear, reflects the polymerization process of PFOS, although the extent of the absorbance variation is very small (0.026–0.055). The absorbance variation of the NIR bands at about 5300, 5164 and 4829 $cm^{-1}$ has been examined in detail and the results may be summarized as follows.

The absorbance variation of the 5164 $cm^{-1}$ band, which is assigned to the combination (so-called $\nu_2 + \nu_3$) mode of a water molecule, occurs in a two-step process. In the first 12 min, the absorbance of this band rapidly decreases, while after this initial step it increases exponentially until finally becoming constant. Variation of the absorption for the 4829 $cm^{-1}$ band coming from the combination mode ($\nu + 2\delta$) of the alcohol OH group also occurs in a two-step process. In the first 12 min, the absorbance of the 4829 $cm^{-1}$ band rapidly increases and in the second step it also increases exponentially until it finally becomes constant. These observations obviously reflect the polymerization process of PFOS in alcohol. That is, for absorbance variation of the 5164 $cm^{-1}$ band, the rapid decrease in absorbance in the initial step implies that water molecules are consumed in the hydrolysis reaction, while the exponential increase in absorbance in the second step implies that water molecules are released as a consequence of the condensation reaction between the silanol groups. For the absorbance variation of the band at 4829 $cm^{-1}$, the rapid increase in intensity in the initial step implies the release of methanol as a consequence of hydrolysis, followed by a slow exponential increase in the second step, also as the consequence of hydrolysis. For these time-dependent absorbance data, a kinetics analysis was carried out and the reaction rate constant for each step was calculated.

2D NIR correlation spectral maps were calculated from the absorbance data, time-resolved over the two step process. These correlation maps also reflect the polymerization process. In particular, in the asynchronous correlation maps, the presence of two species of silanol groups (i.e. weakly associated and associated SiOH groups) was assumed and their behavior was discussed.

**Acknowledgement** We wish to thank K. Ozaki, Department of Chemistry, School of Science, Kansei Gakuin University, for his generous offer of the program (2D-Pocha) for generalized 2D correlation spectroscopy.

## References

1. Johanson OK, Stark FO, Vogel GE, Fleischmann RM (1967) J Compos Mater 1:278
2. Kwei TK (1965) J Polym Sci A 3:3229
3. Erickson PW, Plueddemann EP (1974) In: Brautman LJ, Krock RH (eds) Composite materials, vol. 6. Academic, New York, p 1
4. Rosen MR (1978) J Coating Technol 50:70
5. Dibenedetto AT, Nicolais L, Ambrosi L, Groeger J (1986) In: Ishida H, Koenig JL (eds) Composite interfaces. Elsevier, Amsterdam, p 47
6. Ishida H (1985) In: Ed Ishida, H Molecular characterization of composite interfaces. Plenum, New York, p 25
7. Lee LH (1968) J Colloid Interface Sci 27:751
8. Ishida H, Koenig JL (1978) J Colloid Interface Sci 64:555

9. Shimizu I, Okabayashi H, Taga K, Yoshino A, Nishio E, O'Connor CJ (1997) Vib Spectrosc 14:125
10. Vrancken KC, Van Der Voort P, Gillis-D'Hamers I, Vansant EF, Grobet P (1992) J Chem Soc Faraday Trans 88:3197
11. Jönsson B, Lindman B, Holmberg K, Kronberg B (1998) In: Surfactants and polymers in aqueous solution. Wiley, Chichester, p 31
12. Ogasawaara T, Nara A, Okabayashi H, Nishio E, O'Connor CJ (1999) App Spectrosc (submitted)
13. Noda I (1986) Bull Am Phys Soc 31: 520
14. Noda I (1989) J Am Chem Soc 111:8116
15. Noda I (1990) Appl Spectrosc 44:550
16. Noda I (1993) Appl Spectrosc 47:1329
17. Ozaki Y, Liu Y, Noda I (1997) Appl Spectrosc 51:526
18. Ozaki Y, Noda I (1996) J Near-Infrared Spectrosc 4:85
19. Marcott C, Noda I, Dowrey AE (1991) Anal Chem Acta 250:131
20. Reynolds N (1991) Adv Mater 3:614
21. Gregorius VG, Chao GL, Toriumi HI, Palmer RA (1991) Chem Phys Lett 179:491
22. Palmer RA, Manning CJ, Chao JL, Noda I, Dowrey AE, Marcott C (1991) Appl Spectrosc 45:12
23. Brinker CJ, Keefer KD, Schaefer DW, Ashley CS (1982) J Non-Cryst Solids 48:47
24. Sabata A, Van Ooij WJ, Koch RJ (1993) J Adhes Sci Technol 11:1153
25. Papirer E, Balard H (1990) J Adhes Sci Technol 41:357
26. Vrancken KC, DeCoster L, Van Der Voort P, Grobet J, Vansant EF (1995) J Colloid Interface Sci 170:71
27. Kato M, Taniguchi Y, Sawamura S, Suzuki K (1992) In: Maeno N, Endoh T (eds) Physics and Chemistry of ice. Hokkaido University Press, Sapporo p 83
28. Nishio E, Ikuta N, Okabayashi H, Hannah RW (1990) Appl Spectrosc 44:614
29. Ogasawara T, Izawa K, Hattori N, Okabayashi H, O'Connor CJ (1999) Colloid Polym Sci 278:293
30. Shih PTK, Koenig JL (1975) Mater Sci Eng 20:145
31. (a) Batuev MI, Shostakovskii MF, Belyaev VI, Matvecva AD, Dubrova EW (1954) Dokl Akad Nauk SSSR 95:531; (b) Chem Abstr (1955) 49:6089
32. Benesi HA, Jones AC (1959) J Phys Chem 63:179
33. Richards RE, Thompson HW (1949) J Chem Soc 124